View metadata, citation and similar papers at core.ac.uk
brought to you by CORE
provided by IUPUIScholarWorks

DR. NICKOLAY BRUSTOVETSKY (Orcid ID : 0000-0002-6564-2560)

Article type : Original Article

Accepted Article

Mutant Huntingtin Fails to Directly Impair Brain Mitochondria

James Hamilton[1], Tatiana Brustovetsky[1], and Nickolay Brustovetsky[1,2]

Department of Pharmacology and Toxicology[1], and Stark Neurosciences Research Institute[2], Indiana University School of Medicine, Indianapolis, IN

Running title: Mutant huntingtin does not damage mitochondria

Correspondence: Dr. Nickolay Brustovetsky, Ph.D.
Department of Pharmacology and Toxicology
Indiana University School of Medicine
635 Barnhill Dr., Medical Science Building 547
Indianapolis, IN 46202
Phone 317-278-9229
Fax 317-274-7714
e-mail nbrous@iu.edu
ORCID: 0000-0002-6564-2560

Keywords: Huntington's disease, mitochondria, respiration, mitochondrial membrane potential, calcium, reactive oxygen species

Abbreviations

mHtt, mutant huntingtin; Htt, wild-type huntingtin; HD, Huntington's disease; ROS, reactive oxygen species; 2,4-DNP, 2,4-dinitrophenol; polyQ, poly-glutamine; WT, wild-type; EGTA, ethylene glycol tetraacetic acid; BSA, bovine serum albumin; TPP^+, tetraphenylphosphonium; CII, Complex II, 70 kDa subunit; OMM, outer mitochondrial membrane; GST, glutathione *S*-transferase; RRID, Research Resource Identifier

---

This is the author's manuscript of the article published in final edited form as:

Hamilton, J., Brustovetsky, T., & Brustovetsky, N. (2019). Mutant Huntingtin Fails to Directly Impair Brain Mitochondria. Journal of Neurochemistry, 0(ja). https://doi.org/10.1111/jnc.14852

Accepted Article

Abstract

Although the mechanisms by which mutant huntingtin (mHtt) results in Huntington's disease (HD) remain unclear, mHtt-induced mitochondrial defects were implicated in HD pathogenesis. The effect of mHtt could be mediated by transcriptional alterations, by direct interaction with mitochondria, or by both. In the present study, we tested a hypothesis that mHtt directly damages mitochondria. To test this hypothesis, we applied brain cytosolic fraction from YAC128 mice, containing mHtt, to brain nonsynaptic and synaptic mitochondria from wild-type (WT) mice and assessed mitochondrial respiration with a Clark-type oxygen electrode, membrane potential and Ca^{2+} uptake capacity with tetraphenylphosphonium (TPP^+)- and Ca^{2+}-sensitive electrodes, respectively, and, ROS production with Amplex Red assay. The amount of mHtt bound to mitochondria following incubation with mHtt-containing cytosolic fraction was greater than the amount of mHtt bound to brain mitochondria isolated from YAC128 mice. Despite mHtt binding to WT mitochondria, no abnormalities in mitochondrial functions were detected. This is consistent with our previous results demonstrating the lack of defects in brain mitochondria isolated from R6/2 and YAC128 mice. This, however, could be due to partial loss of mitochondrially bound mHtt during the isolation procedure. Consequently, we increased the amount of mitochondrially bound mHtt by incubating brain nonsynaptic and synaptic mitochondria isolated from YAC128 mice with mHtt-containing cytosolic fraction. Despite enrichment of YAC128 brain mitochondria with mHtt, mitochondrial functions (respiration, membrane potential, ROS production, Ca^{2+} uptake capacity) remained unchanged. Overall, our results suggest that mHtt does not directly impair mitochondrial functions, arguing against the involvement of this mechanism in HD pathogenesis.

INTRODUCTION

Huntington's disease (HD) is a fatal hereditary neurodegenerative disorder that is characterized by progressively declining motor and cognitive capabilities. HD is linked to a mutation in a single gene encoding the huntingtin protein (Htt), a 350 kDa protein that, when mutated, contains an elongated poly-glutamine (polyQ) stretch at a site near the N-terminus (MacDonald *et al.* 1993). In healthy individuals, the polyQ tract in Htt contains less than 35 glutamines (Bates *et al.* 2015). In HD patients, the mutant huntingtin protein (mHtt) with pathologically expanded polyQ stretch leads to striatal and cortical degeneration, and subsequently to HD progression and development of HD symptoms. Despite the identification of the genetic mutation linked to HD, the mechanisms by which mHtt exerts its

This article is protected by copyright. All rights reserved.

harmful effects are not clear. However, bioenergetic abnormalities, augmented reactive oxygen species (ROS) production, and defects in mitochondrial Ca^{2+} handling have been implicated as possible factors contributing to HD pathogenesis.

It has been previously suggested that there might be aberrations in mitochondrial respiration and abnormalities in Ca^{2+} handling in mitochondria from HD mice and HD cell models (Tabrizi *et al.* 2000;Panov *et al.* 2002;Choo *et al.* 2004;Fernandes *et al.* 2007;Lim *et al.* 2008;Kim *et al.* 2011;Aidt *et al.* 2013;Damiano *et al.* 2013). However, in our previous studies, we did not find any evidence for deleterious effects of mHtt on Ca^{2+} handling or oxidative metabolism in brain mitochondria isolated from R6/2 or YAC128 mice (Hamilton *et al.* 2015;Pellman *et al.* 2015;Hamilton *et al.* 2016;Hamilton *et al.* 2017). Wild-type as well as mutant Htt interact with the outer mitochondrial membrane and are not transported into mitochondria (Choo *et al.* 2004;Orr *et al.* 2008). Consistent with previous reports (Choo *et al.* 2004;Orr *et al.* 2008), we showed that mHtt remains attached to mitochondria during the isolation procedure, but whether the remaining attached mHtt is sufficient for inducing mitochondrial defects was not clear. It was possible that some mHtt was washed out from the mitochondria during the isolation procedure and this might explain the lack of mitochondrial defects in our previous experiments (Hamilton *et al.* 2015;Pellman *et al.* 2015;Hamilton *et al.* 2016;Hamilton *et al.* 2017). It was also unclear whether mitochondria from HD mice are predisposed to mHtt-induced impairment or whether mHtt could acutely damage mitochondria from WT animals.

The two major objectives of the current study were to test (i) whether mHtt can directly damage WT mitochondria and (ii) whether enrichment of HD mitochondria with mHtt will result in detectable mitochondrial defects. In the present study, we assessed respiration, membrane potential, ROS production, and Ca^{2+} handling of brain mitochondria isolated from YAC128 and WT mice following acute application of concentrated cytosolic fraction containing mHtt. We found that despite mHtt association with isolated WT mitochondria, there were no abnormalities in mitochondrial respiration, membrane potential, ROS production, or Ca^{2+} uptake capacity. Acute application of mHtt to brain mitochondria isolated from YAC128 mice increased the total amount of mHtt bound to mitochondria, but failed to degrade mitochondrial functions. Consequently, consistent with results from our previous studies, we found no evidence to suggest that mHtt directly and acutely damages mitochondria.

This article is protected by copyright. All rights reserved.

Accepted Article

Accepted Article

MATERIALS and METHODS

Materials

Pyruvate, malate, ethylene glycol tetraacetic acid (EGTA; Cat# E4378), ADP (Cat# A5285), oligomycin (Cat# 75351) and 2,4-dinitrophenol (Cat# D198501) were purchased from Sigma (St. Louis, MO, USA). Tetraphenylphosphonium chloride (Cat# 88060) was from Fluka (Buchs, Switzerland). Percoll (Cat# 17089101) was from GE Healthcare Bio-Sciences (Pittsburgh, PA, USA). Bovine serum albumin (BSA), free from free fatty acids (Cat# 152401), was from MP Biomedicals (Irvine, CA, USA). All materials were purchased no more than 6 months before use.

Animals

All procedures with animals were performed in accordance with the Indiana University School of Medicine Institutional Animal Care and Use Committee approved protocol (# 11385 MD/R). The study was not pre-registered. No randomization was performed to allocate mice in the study. Wild-type FVB/NJ (RRID: IMSR_JAX:001800) mice and transgenic HD YAC128 (RRID: IMSR_JAX:004938) mice of both sexes were used in this study. Breeding pairs of mice were purchased from Jackson Laboratories (Bar Harbor, ME, USA) and breeding colonies were established in the Laboratory Animals Research Center (LARC) at Indiana University School of Medicine, Indianapolis, IN, USA. Male YAC128 mice were bred with female FVB/NJ mice (background strain). Every mouse was genotyped and weighed 19-25g at 2-4 months of age. The mice were housed under standard conditions with free access to food and water. All mice were housed in polycarbonate cages, 3 mice per cage. For our experiments, we used 2-4-month-old YAC128 mice and their wild-type (WT) littermates. Sixty-three FVB/NJ mice and 66 YAC128 mice were used in our study; we used all animals initially taken in the experiment and did not exclude any animal from our study. The total number of animals used in this study was 129. There is evidence that sex hormones may influence mitochondrial functions (Gaignard *et al.* 2017). However, HD affects men and women equally (Novak and Tabrizi 2010;World Health Organization 2016). Therefore, throughout this study, mice of both sexes were used. Mitochondria from male and female WT and YAC128 mice were used simultaneously in experiments. YAC128 mice express full-length human mHtt, including upstream and downstream regulatory elements, containing a polyglutamine (polyQ) region of 128 glutamines. In our study, one investigator was responsible for maintaining the breeding colonies of YAC128 and FVB/NJ mice, preparing

This article is protected by copyright. All rights reserved.

cytosolic fractions, and isolating mitochondria. Then, another investigator conducted the experiments with these fractions and mitochondria without knowing the identity of these materials. Data were analyzed only by the investigator who conducted the experiments.

Genotyping

All offspring used for experiments were genotyped using a PCR assay on tail DNA. PCR of tail DNA was performed according to the protocol provided by Jackson Laboratories with oligonucleotide primers oIMR6533 (GGCTGAGGAAGCTGAGGAG) and TmoIMR1594 (CCGCTCAGGTTCTGCTTTTA) (Invitrogen, Carlsbad, CA, USA). The PCR reaction mixture consisted of 1μl DNA template and 24μl Platinum PCR SuperMix (Invitrogen; Cat# 12532024) containing 0.39μM of each primer (Invitrogen) for a total volume of 25μl. Cycling conditions were 5 min at 95°C, and then 35 cycles of 30 s at 95°C, 30 s at 56°C, 60 s at 72°C, followed by 10 min at 72°C. Reaction products were visualized on a 1.2% agarose gel run at 100 V for 60 min with Tris-acetate-EDTA running buffer containing 1X GelRed™ Nucleic Acid Gel Stain (Biotium, Hayward, CA, USA; Cat# 41003).

Isolation of brain nonsynaptic and synaptic mitochondria

Percoll gradient-purified brain nonsynaptic and synaptic mitochondria from 2-4-month-old YAC128 and age-matched wild-type FVB/NJ littermates were isolated as we described previously with some modifications (Sims 1990;Brustovetsky and Brustovetsky 2017). Briefly, unanesthetized mice were euthanized by rapid decapitation using a sharp guillotine, which is an acceptable method for small rodents approved by American Veterinary Medical Association 2013 Guidelines. All procedures using animals were acute, and the animals experienced no pain. Administration of anesthesia impairs key mitochondrial enzymes (Brunner et al., 1975; Nahrwold and Cohen, 1975; Cohen, 1973; Lenaz et al., 1978). Therefore, in order to study mitochondrial respiration, membrane potential, ROS production, and mitochondrial Ca^{2+} uptake, mitochondria were prepared from unanesthetized animals. To prepare nonsynaptic and synaptic mitochondria, brains of three FVB/NJ and YAC128 mice each were used for a single isolation procedure. After brain tissue was homogenized in a 15 ml glass Dounce homogenizer (10 strokes with pestle A, 30 strokes with pestle B) on ice, homogenate was diluted with 30 ml of Isolation Buffer 1 and centrifuged for 10 minutes at 2,400 rpm in a Beckman Avanti J-26XP centrifuge, rotor JA-25.50 (700×g). All procedures were performed at 2-4ºC. After the 1st centrifugation, supernate was centrifuged for 10 minutes at 12,500 rpm (18,900×g) in a Beckman Avanti J-26XP centrifuge, rotor JA-25.50.

This article is protected by copyright. All rights reserved.

Accepted Article

Supernate (cytosolic fraction) was set aside to be concentrated later, and the pellet was resuspended in 35 ml of Isolation Buffer 1 and centrifuged for 10 minutes at 12,500 rpm (18,900×g) in a Beckman Avanti J-26XP centrifuge, rotor JA-25.50. Then, the pellet was resuspended in 5 ml of Isolation Buffer 2. The suspension was layered onto the top of a Percoll gradient (26%/40%) in Beckman Ultra-Clear centrifuge tubes and centrifuged for 28 minutes at 15,500 rpm (41,100×g) in a Beckman Optima L100K ultracentrifuge, bucket rotor SW41Ti. Following this centrifugation, either synaptosomes were collected for isolation of synaptic mitochondria or nonsynaptic mitochondria were collected. Nonsynaptic mitochondria were resuspended in Isolation Buffer 2 and centrifuged for 20 minutes at 15,500 rpm (41,100×g) in a Beckman Optima L100K ultracentrifuge, bucket rotor SW41Ti. The pellet was resuspended in Isolation Buffer 2 and centrifuged again for 20 minutes at 15,500 rpm (41,100×g) in a Beckman Optima L100K ultracentrifuge, bucket rotor SW41Ti. The pellet was collected, resuspended in Isolation Buffer 2, and stored on ice. This was a stock suspension of brain nonsynaptic mitochondria. Synaptic mitochondria were isolated from synaptosomes by nitrogen cavitation using an ice-cold nitrogen cell disruption vessel (Parr Instrument Co., Moline, IL; Cat# 4639). Briefly, the synaptosomes obtained following Percoll gradient (26%/40%) centrifugation were transferred to a beaker on ice and placed into the nitrogen vessel on ice under 1,100 psi for 13 minutes. Then, the ruptured synaptosomes were layered onto another discontinuous Percoll gradient (24%/40%) and centrifuged for 28 minutes at 15,500 rpm (41,100×g) in a Beckman Optima L100K ultracentrifuge, bucket rotor SW41Ti. Synaptic mitochondria were resuspended in Isolation Buffer 2 and centrifuged twice more for 20 minutes each at 15,500 rpm (41,100×g) in a Beckman Optima, L100K ultracentrifuge, bucket rotor SW41Ti exactly as described above for the final two centrifugations of nonsynaptic mitochondria preparation. The pellet was collected, resuspended in Isolation Buffer 2, and the stock suspension of synaptic mitochondria was stored on ice. The composition of isolation buffers was as follows: Isolation Buffer 1: 225 mM mannitol, 75 mM sucrose, 10 mM Hepes, pH 7.4 adjusted with KOH, 0.1 mM EGTA; Isolation Buffer 2: 395 mM sucrose, 0.1 mM EGTA, 10 mM Hepes, pH 7.4; Percoll Buffer: 320 mM sucrose, 1 mM EGTA, 10 mM Hepes, pH 7.4. The Percoll gradients were prepared using Percoll Buffer with corresponding concentrations of added Percoll. It was previously suggested that BSA may interfere with mHtt binding to mitochondria (Panov *et al.* 2003). Therefore, in our experiments with isolated mitochondria, BSA was omitted from all solutions unless otherwise indicated.

This article is protected by copyright. All rights reserved.

Accepted Article

Accepted Article

Preparation of cytosolic fraction

Cytosolic fraction was collected during the mitochondrial isolation procedure and treated with 1μL/mL Benzonase Nuclease (Sigma, St. Louis, MO, USA; Cat# 70664) for 30 minutes before being centrifuged at 4°C for 30 minutes at 35,000 rpm (76,000×g) in a Beckman Optima L100K ultracentrifuge, rotor Type 90 Ti. The supernate was collected and placed into a Spin-X^R UF 500 100k MWCO concentrator (Sigma; Cat# 431481) that had been previously rinsed with isolation buffer according to the manufacturer's instructions. The supernate was centrifuged at 4°C for 25 minutes at 12,600 rpm (14,900×g) in an Eppendorf 5424R centrifuge. Following centrifugation, the supernate was collected from the concentrator, stored in a fresh tube on ice, and used on the same day.

Mitochondrial respiration and membrane potential

Here and in all other experimental procedures, the experimenter was unaware of the animals' group and type of cytosolic fraction applied to mitochondria during experimentation. Our study was exploratory. No exclusion criteria were pre-determined and no animals were excluded from our study. All experiments were performed during the normal working hours. Mitochondrial respiration was measured with a Clark-type oxygen electrode in a tightly sealed 0.4 mL thermostated chamber at 37°C under continuous stirring. Experiments were performed in the standard incubation medium containing 125 mM KCl, 0.5 mM $MgCl_2$, 3 mM KH_2PO_4, 10 mM Hepes, pH 7.4, 10 mM EGTA supplemented with either 3 mM pyruvate plus 1 mM malate or 3 mM succinate plus 3 mM glutamate. The slope of the oxygen electrode trace corresponds to the respiratory rate. Mitochondrial membrane potential was measured in the standard incubation medium at 37°C with a home-made tetraphenylphosphonium (TPP^+) electrode by following TPP^+ distribution between the incubation medium and mitochondria (Kamo *et al.* 1979). A decrease in external TPP^+ concentration corresponds to mitochondrial polarization, whereas an increase in TPP^+ in the incubation medium corresponds to depolarization. The membrane potential was calculated using Nernst equation and assuming mitochondrial matrix volume was 0.9μL/mg protein as we established for isolated brain mitochondria previously (Brustovetsky *et al.* 2005).

Mitochondrial Ca^{2+} uptake capacity

Mitochondrial Ca^{2+} uptake was measured with a home-made miniature Ca^{2+}-selective electrode in a 0.3 mL chamber at 37°C under continuous stirring. Mitochondrial Ca^{2+} uptake was indicated by a decrease in the external Ca^{2+} concentration. The experiments were

This article is protected by copyright. All rights reserved.

performed in the standard incubation medium supplemented with 3 mM pyruvate and 1 mM malate. As described previously, the incubation medium was also supplemented with 0.1 mM ADP and 1μM oligomycin (Chalmers and Nicholls 2003). Ca^{2+} was delivered to mitochondria as 10μM $CaCl_2$ pulses. Data were quantified as Ca^{2+} uptake capacity per mg of mitochondrial protein.

Mitochondrial ROS production

Mitochondrial ROS production was measured as H_2O_2 released from mitochondria and monitored by an Amplex Red assay (Molecular Probes, Eugene, OR, USA; Cat# A22188) in a 0.4 mL thermostated chamber at 37°C under continuous stirring in the standard incubation medium supplemented with either 3 mM pyruvate plus 1 mM malate or 3 mM succinate plus 3 mM glutamate using a Perkin-Elmer LS 55 luminescence spectrophotometer and excitation/emission wavelengths of 550/590 nm as described previously (Votyakova and Reynolds 2001).

Immunoblotting

Brain nonsynaptic mitochondria and cytosolic fractions pretreated with Protease Inhibitor Cocktail (Roche, Indianapolis, IN, USA; Cat# 04693124001) were incubated with NuPAGE LDS sample buffer (Invitrogen, Carlsbad, CA, USA; Cat# B0007) supplemented with a reducing agent at 70°C for 15 min. Tris-acetate gels (3-8%, Invitrogen; Cat# EA0375) were used for electrophoresis. Proteins were transferred to a Hybond-ECL nitrocellulose membrane (Amersham Biosciences, Piscataway, NJ, USA; Cat# RPN78D) following electrophoresis. Blots were incubated at room temperature for 1 h in a blocking solution that consisted of either protein-free blocking buffer (Pierce, Rockford, IL, USA; Cat# 37572) plus 0.15% Triton X-100 or 4% milk, phosphate-buffered saline, pH 7.2, plus 0.15% Triton X-100. After blocking, blots were incubated with either mouse monoclonal anti-polyQ 1C2 (mAb 1574, Millipore, Temecula, CA, USA, 1:1000; RRID:AB_94263), mouse monoclonal anti-Complex II, 70 kDa subunit (Invitrogen, 1:1000; RRID:AB_1501830), or rabbit monoclonal anti-MEK1/2 (Pierce, 1:2000; RRID:AB_10980233). Blots then were incubated with goat anti-mouse IgG or goat anti-rabbit IgG (1:25000; RRID:AB_2338504 or 1:20000; RRID:AB_2313567, respectively) coupled with horseradish peroxidase (Jackson ImmunoResearch Laboratories, West Grove, PA, USA) and developed with Supersignal West Pico chemiluminescent reagents (Pierce; Cat# 32106). Molecular mass marker HiMark

Accepted Article

This article is protected by copyright. All rights reserved.

Pre-stained High Molecular Weight Protein Standard (7μL, Invitrogen; Cat# LC5699) was used to determine molecular masses. Band densities were quantified with NIH ImageJ 1.48v software (http://rsb.info.nih.gov//ij).

Statistics

Power analysis was performed using G*Force software version 3.1.9.2 by Franz Faul, Universitat Kiel, Germany (Faul *et al.* 2007) to establish the sample size necessary to detect a 30% difference between mitochondria treated with a vehicle, WT cytosolic fraction (WT cf) and HD cytosolic fraction (HD cf). We used F test, statistical test ANOVA: repeated measures within factors, *a priori* power analysis, assuming effect size 0.3, alpha 0.05, power (1-beta) 0.8, number of groups – 3 (vehicle-, WT cf- and HD cf-treated mitochondria), number of measurements – 5, total sample size – 15 (number of all measurements). Based on this power analysis, the number of experiments that gives an 80% likelihood (the accepted level in statistical analysis) of detecting 30% difference between three means at the significance level of α=0.05 is 5 biological replicates with 3 technical replicates in each experiment. Data are shown as mean ± SD of indicated number of independent experiments. Statistical analysis of the experimental results consisted of unpaired t-test or one-way ANOVA followed by Bonferroni's *post hoc* test if applicable (GraphPad Prism 4.0, GraphPad Software Inc., San Diego, CA, USA). No assessment of the normality of data was carried out. No test for outliers was conducted and no data points were excluded.

RESULTS

To answer the questions of whether mHtt can directly damage WT mitochondria and whether enrichment of HD mitochondria with exogenous mHtt will result in detectable mitochondrial defects, we prepared concentrated cytosolic fraction from brains of WT and YAC128 mice. Immunoblotting experiments using mHtt-specific monoclonal antibody 1C2 demonstrated the presence of mHtt in cytosolic fraction from YAC128 mice but not from WT animals (Fig. 1A). Further enrichment of cytosolic fraction with mHtt was achieved by the concentrating procedure using a Spin-X^{R} UF 500 100k MWCO concentrator (Sigma) (Fig. 1B). Figure 1E depicts a statistical summary of densitometry with immunoblots exemplified by the representative blot shown in Fig. 1B. The concentrated mHtt-containing cytosolic fraction was applied at 37ºC under gentle shaking to Percoll gradient-purified brain mitochondria from WT and YAC128 mice to assess binding of mHtt to brain mitochondria. Following 5 minutes of incubation with concentrated mHtt-containing cytosolic fraction, mitochondria

This article is protected by copyright. All rights reserved.

Accepted Article

were washed out three times with fresh incubation medium. MEK1/2, a cytosolic marker, was used to assess the removal of cytosolic components from the mitochondrial suspension. Immunoblotting with anti-MEK1/2 antibody confirmed complete removal of cytosolic fraction from mitochondria following three washes (Fig. 1C). Immunoblotting with anti-Complex II, 70 kDa subunit (CII), antibody served as a loading control for mitochondrial samples. The incubation of WT mitochondria with concentrated mHtt-containing cytosolic fraction from YAC128 mice for 5 minutes resulted in binding of mHtt to mitochondria (Fig. 1C). We could detect an mHtt band on the blot following incubation of WT mitochondria with as little as 20μg of cytosolic protein from YAC128 mice (Fig. 1C). Incubation of WT mitochondria with 80μg of cytosolic protein from YAC128 mice resulted in increased binding of mHtt to WT mitochondria. Figure 1F depicts a statistical summary of densitometry of indicated bands represented by the blot shown in Fig. 1C. The amount of mHtt bound to WT mitochondria treated with 80μg of cytosolic protein from YAC128 mice was higher than the amount of mHtt associated with brain mitochondria isolated from YAC128 mice (Fig. 1C). Incubation of brain mitochondria from YAC128 mice for 5 minutes with concentrated cytosolic fraction (80μg of protein) from the same animals also increased mHtt binding to mitochondria (Fig. 1D). However, exposure of mitochondria to increased amount of cytosolic fraction (120μg of protein) and prolonged incubation with cytosolic fraction (15 minutes) did not result in further increased mHtt binding to mitochondria (Fig. 1D). Figure 1G shows a statistical summary of densitometry of selected bands represented by the blot shown in Fig. 1D. Based on immunoblotting assessment, in all subsequent experiments we evaluated mitochondrial functions following the treatment of brain mitochondria for 5 minutes with 80μg of protein of concentrated cytosolic fractions produced from brains of WT or YAC128 mice.

To assess the possible deleterious effect of mHtt on mitochondria, we treated brain mitochondria from WT mice with mHtt-containing brain cytosolic fraction from YAC128 animals and assessed mitochondrial respiration. As a control, we evaluated the effect of vehicle (10μL of Isolation Buffer 1) or the effect of concentrated cytosolic fraction from brains of WT mice, which contained Htt, but not mHtt. We measured mitochondrial respiration with either a combination of Complex I substrates pyruvate (3 mM) and malate (1 mM), or with the Complex II substrate succinate (3 mM) (Fig. 2). In the case of succinate, incubation medium was supplemented with glutamate (3 mM) to stimulate a transaminase reaction that facilitates the removal of oxaloacetate, an endogenous inhibitor of succinate

This article is protected by copyright. All rights reserved.

Accepted Article

dehydrogenase (Wojtczak 1969;Brustovetsky and Dubinsky 2000). We measured basal mitochondrial respiration in the presence of substrates (V_2), respiration in the presence of added cytosolic fraction (V_{cf}), respiration stimulated by ADP (V_3), respiration following ADP depletion (V_4), and uncoupled respiration in the presence of 2,4-dinitrophenol (2,4-DNP, V_{DNP}). Brain mitochondria from WT mice had similar respiratory rates under all conditions tested whether mitochondria were exposed to cytosolic fractions from WT or YAC128 animals (Fig. 2).

In our previous studies, we found no evidence for defects in mitochondria isolated and purified from R6/2 and YAC128 mice. Such findings could be due to a decrease in mitochondrially bound mHtt during the isolation procedure. Therefore, in the present study, we increased the amount of mHtt bound to mitochondria by incubating brain mitochondria isolated from YAC128 mice with mHtt-containing cytosolic fraction. In immunoblotting experiments, we found increased binding of mHtt to mitochondria from YAC128 mice following incubation of these organelles with concentrated cytosolic fraction from the same animals (Fig. 1D, G). However, the enrichment with mHtt did not alter respiration of brain mitochondria from YAC128 mice (Fig. 3).

In addition to mitochondrial respiration, we also analyzed membrane potential ($\Delta\psi$) of brain mitochondria isolated from WT mice following treatment with cytosolic fractions from either YAC128 or WT mice (Fig. 4). Mitochondrial membrane potential was assessed by measuring the distribution of the lipophilic cation tetraphenylphosphonium (TPP^+) across the inner mitochondrial membrane. Similar to experiments with respiration, $\Delta\psi$ was measured with either a combination of Complex I substrates pyruvate (3 mM) and malate (1 mM), or with the Complex II substrate succinate (3 mM) supplemented with glutamate (3 mM). The treatment with mHtt- or Htt-containing cytosolic fractions did not significantly change $\Delta\psi$ (Fig. 4). Similarly, for each substrate type, the responses to ADP were similar in mitochondria exposed to Htt or mHtt (Fig. 4). Consistent with respiration experiments, our data with $\Delta\psi$ measurements suggest that neither Htt nor mHtt directly and acutely alter $\Delta\psi$ in brain mitochondria. We also assessed $\Delta\psi$ of brain mitochondria from YAC128 mice following enrichment with mHtt and found that $\Delta\psi$ was not altered (Fig. 5).

Accepted Article

This article is protected by copyright. All rights reserved.

It has been previously reported that ROS production is augmented in mHtt-expressing cells compared to control cells (Hands *et al.* 2011;Chiang *et al.* 2012). In the current study, we used an Amplex Red Assay to evaluate H_2O_2 production in mitochondria from WT mice treated with mHtt-containing cytosolic fraction. ROS generation was notably lower in mitochondria that were fueled by pyruvate plus malate compared with mitochondria that were incubated with succinate plus glutamate, similar to previously reported data (Pellman *et al.* 2015). However, under both conditions, there was no difference in H_2O_2 generation between WT mitochondria that were treated with mHtt- or Htt-containing cytosolic fractions (Fig 6). We also assessed H_2O_2 production in brain mitochondria from YAC128 mice and found that mHtt enrichment did not alter H_2O_2 production in these mitochondria (Fig. 7).

Mitochondrial Ca^{2+} uptake is critical for the clearance of excessive Ca^{2+} from the cytosol, thus contributing to the maintenance of Ca^{2+} homeostasis inside of cells and to cell survival (Bernardi and Rasola 2007). The amount of Ca^{2+} that can be accumulated by mitochondria is limited by induction of the mitochondrial permeability transition pore (Chalmers and Nicholls 2003). It has been previously reported that mitochondria from HD animal and cell models have decreased Ca^{2+} uptake capacity compared with mitochondria from WT animals and cells (Panov *et al.* 2002;Milakovic *et al.* 2006;Lim *et al.* 2008;Gellerich *et al.* 2008). However, in our previous studies we did not find a decrease in Ca^{2+} uptake capacity in mitochondria from HD mice compared to mitochondria from WT mice (Pellman *et al.* 2015;Hamilton *et al.* 2016;Hamilton *et al.* 2017). In the present study, brain mitochondria isolated from WT mice were treated with mHtt- or Htt-containing cytosolic fractions prior to assessment of mitochondrial Ca^{2+} uptake capacity (Fig. 8). Mitochondria were fueled with a combination of Complex I-linked substrates pyruvate (3 mM) and malate (1 mM), and since it was previously proposed that BSA may displace mHtt from the outer mitochondrial membrane (OMM), precluding the detection of functional difference between mitochondria from HD and WT animals (Panov *et al.* 2003), BSA was omitted from all media. Of note, in our previous study we did not find evidence for mHtt displacement from mitochondria by BSA (Pellman *et al.* 2015). Wild-type mitochondria exposed to mHtt had similar Ca^{2+} uptake capacity compared to WT mitochondria exposed to Htt (Fig 8A, B). In addition, we evaluated Ca^{2+} uptake capacity of mitochondria from YAC128 mice following enrichment with mHtt (Fig. 8C). Ca^{2+} uptake was monitored under the same conditions that were described for experiments with WT mitochondria (Fig. 8A). The Ca^{2+} uptake capacity of brain mitochondria from YAC128 mice was not changed by mHtt enrichment (Fig. 8D).

This article is protected by copyright. All rights reserved.

Accepted Article

Using synaptic mitochondria isolated from both WT and YAC128 mice and exposed to a vehicle or concentrated mHtt-containing cytosolic fraction, we measured respiration, membrane potential, ROS production and Ca^{2+} uptake capacity and obtained results similar to those produced with nonsynaptic mitochondria (Suppl. Figs. 1-4)

DISCUSSION

The possible involvement of mitochondrial dysfunction in the pathogenesis of HD has been investigated since before the causative mutation in HD was even identified (Brennan, Jr. *et al.* 1985). However, the results from studies of mitochondrial functions in HD have been contradictory, and it remains unclear whether mHtt expression results in mitochondrial defects and whether these mitochondrial defects contribute to HD pathogenesis (Brustovetsky 2016). Differences in experimental models of HD used in these studies as well as the wide array of experimental techniques applied by different investigators may account for some of the discrepancies in experimental results. In our previous work, we assessed mitochondrial functions in different mouse models of HD and demonstrated that nonsynaptic and synaptic mitochondria isolated from either whole brains of YAC128 and R6/2 mice or from striata of YAC128 mice had similar respiratory rates, ROS production, and Ca^{2+} uptake capacity compared to mitochondria from WT animals (Pellman *et al.* 2015;Hamilton *et al.* 2015;Hamilton *et al.* 2016;Hamilton *et al.* 2017). Consistent with our results produced with isolated mitochondria, experiments with cultured striatal neurons derived from YAC128 and R6/2 mice and corresponding WT mice indicated that oxidative metabolism and mitochondrial Ca^{2+} handling were not altered in neurons expressing mHtt compared to WT neurons (Pellman *et al.* 2015;Hamilton *et al.* 2015;Hamilton *et al.* 2016). Despite the use of different animal models and experimental techniques, these studies consistently demonstrated the lack of mitochondrial dysfunction in HD samples, arguing against this mechanism as a contributing factor in HD pathogenesis.

In the present study, we evaluated whether the direct application of mHtt to brain mitochondria from WT mice could alter respiration, membrane potential, ROS production, and Ca^{2+} uptake capacity. If mitochondrial dysfunction does, indeed, contribute to HD pathogenesis, such dysfunction could be incited by two mechanisms. Either mHtt indirectly inhibits normal mitochondrial functions by interfering with processes such as transcription

This article is protected by copyright. All rights reserved.

which ultimately results in mitochondrial aberrations (Chiang *et al.* 2012), or mHtt directly damages mitochondria through mechanisms that may include interacting with proteins on the OMM (Yano *et al.* 2014). Our current study tested the latter hypothesis by evaluating the effect of acutely applied mHtt to mitochondria from WT mice.

In an earlier study, Panov et al. found that acute treatment of rat liver mitochondria and human lymphoblast mitochondria with the glutathione *S*-transferase (GST) fusion protein containing a pathological-length polyQ stretch induced more rapid mitochondrial depolarization in response to Ca^{2+} compared with mitochondria incubated with fusion proteins containing a shorter polyQ stretch (Panov *et al.* 2003). Soon after, Puranam et al. reported that pathologic-length polyQ-GST fusion protein directly inhibited ADP-dependent (State 3) respiration and increased the production of ROS in mitochondria isolated from mouse liver (Puranam *et al.* 2006). In these studies, the authors used a polyQ-GST fusion protein containing a pathological-length polyQ stretch (Panov *et al.* 2002;Puranam *et al.* 2006). The use of this artificial construct potentially could lead to artifacts. In our study, we treated isolated brain mitochondria with cytosolic fraction prepared from the brains of YAC128 mice and containing natural human full-length mHtt, which is more physiologically relevant. The lack of direct and acute mHtt effect on brain mitochondria, described in the current paper, is consistent with our previous reports, indicating the lack of defects both in brain mitochondria isolated from HD mice (R6/2 and YAC128) and in mitochondria of cultured neurons from these animals (Pellman *et al.* 2015;Hamilton *et al.* 2015;Hamilton *et al.* 2016;Hamilton *et al.* 2017).

The use of isolated mitochondria as a model system allows for the examination of mitochondrial functions under well-defined conditions. Despite this advantage, there are obvious limitations of using isolated mitochondria. Although, this model allows for the design of straightforward experiments to answer simple questions, it does not and is not intended to completely recapitulate *in vivo* conditions. Isolated mitochondria are removed from their natural environment while being subjected to a harsh isolation procedure. Therefore, it is conceivable that some proteins associated with the OMM could be lost during the isolation procedure. We and others have previously shown that mHtt remains attached to the OMM during mitochondrial isolation (Choo *et al.* 2004;Orr *et al.* 2008;Pellman *et al.* 2015;Hamilton *et al.* 2015). However, it is unclear how much mHtt associated with mitochondria *in vivo* remains attached to the OMM following the isolation procedure. This consideration raises the possibility that, if mHtt does directly interfere with mitochondrial

This article is protected by copyright. All rights reserved.

Accepted Article

functions, then failure to observe such mitochondrial defects in our previous studies may have been due to dissociation of mHtt from the OMM and partial loss of mHtt during mitochondrial isolation. Additionally, considering the lack of dysfunction in WT mitochondria acutely treated with cytosolic fraction from YAC128 mice, one can hypothesize that mitochondria from YAC128 mice may possess some inherent characteristics that make them susceptible to the deleterious effects of mHtt. Consequently, in the current study we analyzed the functions of brain mitochondria from YAC128 mice following enrichment with mHtt. However, despite our stringent efforts, brain mitochondria derived from YAC128 mice and enriched with mHtt did not demonstrate alterations in respiration, membrane potential, ROS production, and Ca^{2+} uptake capacity compared to mitochondria from YAC128 mice treated with Htt-containing cytosolic fraction.

In an elegant study, Yano et al. (2014) demonstrated an mHtt-induced decrease in mitochondrial protein import (Yano *et al.* 2014). However, in that study Yano et al. did not investigate whether inhibition of protein import led to decreased expression of nuclear-encoded mitochondrial proteins. We previously assessed the level of expression of randomly chosen nuclear-encoded proteins in mitochondria of WT and HD mice and did not find any difference (Hamilton *et al.* 2015;Hamilton *et al.* 2016). Consistent with these previous studies, the lack of altered protein expression in mitochondria from WT and HD mice and striatal cells has been reported by other groups (Orr *et al.* 2008; Milakovic and Johnson 2005). Moreover, despite reporting inhibition of mitochondrial protein import, Yano et al. did not find any sign of mitochondrial respiratory dysfunction (Yano *et al.* 2014), which is consistent with our findings (Hamilton *et al.* 2015;Hamilton *et al.* 2016). In the current study, based on our previously published results and data from other groups, we decided not to investigate mitochondrial protein import further.

Overall, our current data with mHtt acutely applied to isolated brain mitochondria and previously published data with whole-brain and striatal mitochondria do not provide evidence for mHtt-induced mitochondrial respiratory deficiency, abnormal ROS production, and defects in mitochondrial Ca^{2+} handling (Pellman *et al.* 2015;Hamilton *et al.* 2015;Hamilton *et al.* 2016;Hamilton *et al.* 2017). The lack of alterations in respiration, membrane potential, ROS production, and Ca^{2+} uptake by brain mitochondria acutely exposed to mHtt suggests that mHtt does not directly impair mitochondria. Consequently, mHtt neurotoxicity most likely could be mediated by mechanisms unrelated to overt mitochondrial defects, but linked

This article is protected by copyright. All rights reserved.

Accepted Article

Accepted Article

to the events such as oxidative stress associated with elevated NAD(P)H oxidase activity (Brennan *et al.* 2009;Tarafdar and Pula 2018), alterations in cholesterol metabolism (Trushina *et al.* 2014), aberrant mitochondrial trafficking (Trushina *et al.* 2004;Shirendeb *et al.* 2012), or metabolic reprograming to preferential oxidation of fatty acids (Polyzos *et al.* 2019). Therefore, it is conceivable that mitochondrial impairment, if it is involved in HD pathology, may exist as a secondary process downstream of mHtt-induced deleterious changes in other cellular functions.

ACKNOWLEDGEMENTS

This study was supported by National Institutes of Health grant R01 NS098772 and in part by a grant from Indiana Traumatic Spinal Cord & Brain Injury Research Fund to N.B.

CONFLICT OF INTEREST

The authors declare that they do not have conflict of interest.

Open Science Badges

This article has received a badge for ***Open Materials*** because it provided all relevant information to reproduce the study in the manuscript. The complete Open Science Disclosure form for this article can be found at the end of the article. More information about the Open Practices badges can be found at https://cos.io/our-services/open-science-badges/.

This article is protected by copyright. All rights reserved.

REFERENCES

Aidt F. H., Nielsen S. M., Kanters J., Pesta D., Nielsen T. T., Norremolle A., Hasholt L., Christiansen M. and Hagen C. M. (2013) Dysfunctional mitochondrial respiration in the striatum of the Huntington's disease transgenic R6/2 mouse model. *PLoS. Curr.* **5**.

Bates G. P., Dorsey R., Gusella J. F., Hayden M. R., Kay C., Leavitt B. R., Nance M., Ross C. A., Scahill R. I., Wetzel R., Wild E. J. and Tabrizi S. J. (2015) Huntington disease. *Nat. Rev. Dis. Primers.* **1,** 15005.

Bernardi P. and Rasola A. (2007) Calcium and cell death: the mitochondrial connection. *Subcell. Biochem.* **45,** 481-506.

Brennan A. M., Suh S. W., Won S. J., Narasimhan P., Kauppinen T. M., Lee H., Edling Y., Chan P. H. and Swanson R. A. (2009) NADPH oxidase is the primary source of superoxide induced by NMDA receptor activation. *Nat. Neurosci.* **12,** 857-863.

Brennan W. A., Jr., Bird E. D. and Aprille J. R. (1985) Regional mitochondrial respiratory activity in Huntington's disease brain. *J. Neurochem.* **44,** 1948-1950.

Brunner E. A., Cheng S. C., and Berman M. L. (1975) Effects of anesthesia on intermediary metabolism. *Ann. Rev. Med.* **26,** 391-401.

Brustovetsky N. (2016) Mutant Huntingtin and Elusive Defects in Oxidative Metabolism and Mitochondrial Calcium Handling. *Mol. Neurobiol.* **53,** 2944-2953.

Brustovetsky N. and Brustovetsky T. (2017) Monitoring of permeability transition pore openings in isolated individual brain mitochondria., in *Techniques to investigate mitochondrial fucntion in neurons,* (Strack S. and Usachev Y., eds), pp. 199-210. New York.

Brustovetsky N. and Dubinsky J. M. (2000) Dual responses of CNS mitochondria to elevated calcium. *J. Neurosci.* **20,** 103-113.

Brustovetsky T., Shalbuyeva N. and Brustovetsky N. (2005) Lack of manifestations of diazoxide/5-hydroxydecanoate-sensitive KATP channel in rat brain nonsynaptosomal mitochondria. *J. Physiol* **568,** 47-59.

Chalmers S. and Nicholls D. G. (2003) The relationship between free and total calcium concentrations in the matrix of liver and brain mitochondria. *J. Biol. Chem.* **278,** 19062-19070.

Chiang M. C., Chern Y. and Huang R. N. (2012) PPARgamma rescue of the mitochondrial dysfunction in Huntington's disease. *Neurobiol. Dis.* **45,** 322-328.

Choo Y. S., Johnson G. V., MacDonald M., Detloff P. J. and Lesort M. (2004) Mutant huntingtin directly increases susceptibility of mitochondria to the calcium-induced permeability transition and cytochrome c release. *Hum. Mol. Genet.* **13,** 1407-1420.

Cohen P. J. (1973) Effect of anesthetics on mitochondrial function. *Anesthesiology* **39**, 153-164.

Damiano M., Diguet E., Malgorn C., D'Aurelio M., Galvan L., Petit F., Benhaim L., Guillermier M., Houitte D., Dufour N., Hantraye P., Canals J. M., Alberch J., Delzescaux T.,

This article is protected by copyright. All rights reserved.

Accepted Article

Accepted Article

Deglon N., Beal M. F. and Brouillet E. (2013) A role of mitochondrial complex II defects in genetic models of Huntington's disease expressing N-terminal fragments of mutant huntingtin. *Hum. Mol. Genet.* **22,** 3869-3882.

Faul F., Erdfelder E., Lang A. G. and Buchner A. (2007) G*Power 3: a flexible statistical power analysis program for the social, behavioral, and biomedical sciences. *Behav. Res. Methods* **39,** 175-191.

Fernandes H. B., Baimbridge K. G., Church J., Hayden M. R. and Raymond L. A. (2007) Mitochondrial sensitivity and altered calcium handling underlie enhanced NMDA-induced apoptosis in YAC128 model of Huntington's disease. *J. Neurosci.* **27,** 13614-13623.

Gaignard P., Liere P., Therond P., Schumacher M., Slama A. and Guennoun R. (2017) Role of Sex Hormones on Brain Mitochondrial Function, with Special Reference to Aging and Neurodegenerative Diseases. *Front Aging Neurosci.* **9,** 406.

Gellerich F. N., Gizatullina Z. Z., Nguyen H. P., Trumbeckaite S., Vielhaber S., Seppet E., Zierz S., Landwehrmeyer B., Ries O., von Hoersten S. and Striggow F. (2008) Impaired regulation of brain mitochondria by extramitochondrial Ca2+ in transgenic Huntington disease rats. *J. Biol. Chem.* **283,** 30715-30724.

Hamilton J., Brustovetsky T. and Brustovetsky N. (2017) Oxidative metabolism and Ca2+ handling in striatal mitochondria from YAC128 mice, a model of Huntington's disease. *Neurochem. Int.* **109,** 24-33.

Hamilton J., Pellman J. J., Brustovetsky T., Harris R. A. and Brustovetsky N. (2015) Oxidative metabolism in YAC128 mouse model of Huntington's disease. *Hum. Mol. Genet.* **24,** 4862-4878.

Hamilton J., Pellman J. J., Brustovetsky T., Harris R. A. and Brustovetsky N. (2016) Oxidative metabolism and Ca2+ handling in isolated brain mitochondria and striatal neurons from R6/2 mice, a model of Huntington's disease. *Hum. Mol. Genet.* **25,** 2762-2775.

Hands S., Sajjad M. U., Newton M. J. and Wyttenbach A. (2011) In vitro and in vivo aggregation of a fragment of huntingtin protein directly causes free radical production. *J. Biol. Chem.* **286,** 44512-44520.

Kamo N., Muratsugu M., Hongoh R. and Kobatake Y. (1979) Membrane potential of mitochondria measured with an electrode sensitive to tetraphenyl phosphonium and relationship between proton electrochemical potential and phosphorylation potential in steady state. *J. Membr. Biol.* **49,** 105-121.

Kim S. H., Thomas C. A., Andre V. M., Cummings D. M., Cepeda C., Levine M. S. and Ehrlich M. E. (2011) Forebrain striatal-specific expression of mutant huntingtin protein in vivo induces cell-autonomous age-dependent alterations in sensitivity to excitotoxicity and mitochondrial function. *ASN. Neuro.* **3,** e00060.

Lenaz G., Curatola G., Mazzanti L., Parenti-Castelli G., and Bertoli E. (1978) Effects of general anesthetics on lipid protein interactions and ATPase activity in mitochondria. *Biochem. Pharmacol.* **27,** 2835-2844.

This article is protected by copyright. All rights reserved.

Accepted Article

Lim D., Fedrizzi L., Tartari M., Zuccato C., Cattaneo E., Brini M. and Carafoli E. (2008) Calcium homeostasis and mitochondrial dysfunction in striatal neurons of Huntington disease. *J. Biol. Chem.* **283,** 5780-5789.

MacDonald M. E., Ambrose C. M., Duyao M. P., Myers R. H., Lin C., Srinidhi L., Barnes G., Taylor S. A., James M., Groot N., MacFarlane H., Jenkins B., Anderson M. A., Wexler N. S., Gusella J. F., Bates G. P., Baxendale S., Hummerich H., Kirby S., North M., Youngman S., Mott R., Zehetner G., Sedlacek Z., Poustka A., Frischauf A. M., Lehrach H., Buckler A. J., Church D., Doucette-Stamm L., O'Donovan M. C., Riba-Ramirez L., Shah M., Stanton V. P., Strobel S. A., Draths K. M., Wales J. L., Dervan P., Housman D. E., Altherr M., Shiang R., Thompson L., Fielder T., Wasmuth J. J., Tagle D., Valdes J., Elmer L., Allard M., Castilla L., Swaroop M., Blanchard K., Collins F. S., Snell R., Holloway T., Gillespie K., Datson N., Shaw D. and Harper P. S. (1993) A novel gene containing a trinucleotide repeat that is expanded and unstable on Huntington's disease chromosomes. *Cell* **72,** 971-983.

Milakovic T., Quintanilla R. A. and Johnson G. V. (2006) Mutant huntingtin expression induces mitochondrial calcium handling defects in clonal striatal cells: functional consequences. *J. Biol. Chem.* **281,** 34785-34795.

Nahrwold M. L. and Cohen P. J. (1975) Anesthetics and mitochondrial respiration. *Clin. Anesth.* **11,** 25-44.

Novak M. J. and Tabrizi S. J. (2010) Huntington's disease. *BMJ* **340,** 34-40.

Orr A. L., Li S., Wang C. E., Li H., Wang J., Rong J., Xu X., Mastroberardino P. G., Greenamyre J. T. and Li X. J. (2008) N-terminal mutant huntingtin associates with mitochondria and impairs mitochondrial trafficking. *J. Neurosci.* **28,** 2783-2792.

Panov A. V., Burke J. R., Strittmatter W. J. and Greenamyre J. T. (2003) In vitro effects of polyglutamine tracts on Ca2+-dependent depolarization of rat and human mitochondria: relevance to Huntington's disease. *Arch. Biochem. Biophys.* **410,** 1-6.

Panov A. V., Gutekunst C. A., Leavitt B. R., Hayden M. R., Burke J. R., Strittmatter W. J. and Greenamyre J. T. (2002) Early mitochondrial calcium defects in Huntington's disease are a direct effect of polyglutamines. *Nat. Neurosci.* **5,** 731-736.

Pellman J. J., Hamilton J., Brustovetsky T. and Brustovetsky N. (2015) Ca(2+) handling in isolated brain mitochondria and cultured neurons derived from the YAC128 mouse model of Huntington's disease. *J. Neurochem.* **134,** 652-667.

Polyzos A. A., Lee D. Y., Datta R., Hauser M., Budworth H., Holt A., Mihalik S., Goldschmidt P., Frankel K., Trego K., Bennett M. J., Vockley J., Xu K., Gratton E. and McMurray C. T. (2019) Metabolic Reprogramming in Astrocytes Distinguishes Region-Specific Neuronal Susceptibility in Huntington Mice. *Cell Metab* **29,** 1-16.

Puranam K. L., Wu G., Strittmatter W. J. and Burke J. R. (2006) Polyglutamine expansion inhibits respiration by increasing reactive oxygen species in isolated mitochondria. *Biochem. Biophys. Res. Commun.* **341,** 607-613.

Shirendeb U. P., Calkins M. J., Manczak M., Anekonda V., Dufour B., McBride J. L., Mao P. and Reddy P. H. (2012) Mutant huntingtin's interaction with mitochondrial protein Drp1

This article is protected by copyright. All rights reserved.

Accepted Article

impairs mitochondrial biogenesis and causes defective axonal transport and synaptic degeneration in Huntington's disease. *Hum. Mol. Genet.* **21,** 406-420.

Sims N. R. (1990) Rapid isolation of metabolically active mitochondria from rat brain and subregions using Percoll density gradient centrifugation. *J. Neurochem.* **55,** 698-707.

Tabrizi S. J., Workman J., Hart P. E., Mangiarini L., Mahal A., Bates G., Cooper J. M. and Schapira A. H. (2000) Mitochondrial dysfunction and free radical damage in the Huntington R6/2 transgenic mouse. *Ann. Neurol.* **47,** 80-86.

Tarafdar A. and Pula G. (2018) The Role of NADPH Oxidases and Oxidative Stress in Neurodegenerative Disorders. *Int. J. Mol. Sci.* **19**.

Trushina E., Canaria C. A., Lee D. Y. and McMurray C. T. (2014) Loss of caveolin-1 expression in knock-in mouse model of Huntington's disease suppresses pathophysiology in vivo. *Hum. Mol. Genet.* **23,** 129-144.

Trushina E., Dyer R. B., Badger J. D., Ure D., Eide L., Tran D. D., Vrieze B. T., Legendre-Guillemin V., McPherson P. S., Mandavilli B. S., Van H. B., Zeitlin S., McNiven M., Aebersold R., Hayden M., Parisi J. E., Seeberg E., Dragatsis I., Doyle K., Bender A., Chacko C. and McMurray C. T. (2004) Mutant huntingtin impairs axonal trafficking in mammalian neurons in vivo and in vitro. *Mol. Cell Biol.* **24,** 8195-8209.

Votyakova T. V. and Reynolds I. J. (2001) DeltaPsi(m)-Dependent and -independent production of reactive oxygen species by rat brain mitochondria. *J. Neurochem.* **79,** 266-277.

Wojtczak A. B. (1969) Inhibitory action of oxaloacetate on succinate oxidation in rat-liver mitochondria and the mechanism of its reversal. *Biochim. Biophys. Acta* **172,** 52-65.

World Health Organization (2016) Human Genomics in Global Health: Genes and human disease. www.who.int/genomics/public/geneticdiseases/en/index2.html#HD

Yano H., Baranov S. V., Baranova O. V., Kim J., Pan Y., Yablonska S., Carlisle D. L., Ferrante R. J., Kim A. H. and Friedlander R. M. (2014) Inhibition of mitochondrial protein import by mutant huntingtin. *Nat. Neurosci.* **17,** 822-831.

This article is protected by copyright. All rights reserved.

Accepted Article

Figure Legends

Figure 1. Detection of mHtt bound to WT and YAC128 nonsynaptic mitochondria following incubation with brain cytosolic fraction from YAC128 mice. In **A**, mHtt was detected with mHtt-specific monoclonal antibody 1C2 as a single 350 kDa band in brain cytosolic fraction from YAC128 but not WT mice. Here and in other panels (**B**-**D**), MEK1/2 was used as a cytosolic marker, indicating the absence of cytosolic contamination in mitochondrial fraction, and Complex II, 70 kDa subunit (CII) was used as a mitochondrial marker as control for loading. In **B**, mHtt enrichment in brain cytosolic fraction from YAC128 mice after concentrating with Spin-X^R UF 500 100k MWCO concentrators (Sigma). In **C**, mHtt presence in brain mitochondrial fraction from YAC128 mice (YAC) and binding of mHtt to WT mitochondria. WT mitochondria were incubated with either 20 or 80μg of protein of concentrated YAC128 brain cytosolic fraction for 5 minutes and then washed out three times. In **D**, enrichment of YAC128 mitochondria with mHtt following incubation with either 80 or 120μg of protein of concentrated YAC128 brain cytosolic fraction for 5 or 15 minutes. In **E**, the statistical summary of densitometry of mHtt bands obtained with 1C2 antibody in cytosolic fractions before and after concentrating procedure. Data are mean±SD, n=4 separate independent mitochondrial preparations, ***p*<0.01 comparing the level of mHtt in YAC128 cytosolic fraction before and after concentrating procedure. In **F** and **G**, the statistical summaries of densitometry of mHtt bands obtained with 1C2 antibody in mitochondrial samples before and after treatment with concentrated mHtt-containing cytosolic fraction. Mutant Htt band intensities were normalized to respective CII signals. Data are mean±SD, n=4 separate independent mitochondrial preparations, **p*<0.05 comparing the level of mHtt bound to WT mitochondria treated with 80μg of concentrated mHtt-containing cytosolic fraction and to untreated YAC128 mitochondria. ***p*<0.01 comparing the level of mHtt bound to WT mitochondria treated with either 20 or 80μg of concentrated mHtt-containing cytosolic fraction (**F**); ***p*<0.01 comparing the level of mHtt bound to untreated YAC128 mitochondria and YAC128 mitochondria treated with either 80 or 120μg of concentrated mHtt-containing cytosolic fraction (**G**).

Figure 2. Respiratory activity of brain nonsynaptic mitochondria isolated from WT mice following acute application of brain cytosolic fractions from WT or YAC128 animals. In **A** and **C**, representative traces of oxygen consumption by mitochondria treated with either vehicle (green traces), WT concentrated cytosolic fraction (WT cf, blue traces), or YAC128 concentrated cytosolic fraction (HD cf, red traces). Where indicated, ADP (250μM in **A**, 150μM in **C**), 2,4-dinitrophenol (2,4-DNP, 60μM), and vehicle (10μL of Isolation Medium 1), or WT or YAC128 cytosolic fractions (WT cf or HD cf, 80μg of protein) were added to mitochondria. The incubation medium was supplemented with either 3 mM pyruvate (pyr) and 1 mM malate (mal) (**A**) or 3 mM succinate (succ) and 3 mM glutamate (glu) (**C**). In **B** and **D**, the statistical summary of respiratory rates of mitochondria incubated with either pyruvate plus malate (**B**) or succinate plus glutamate (**D**). Data are mean±SD, n=5 separate independent mitochondrial preparations.

Figure 3. Respiratory activity of brain nonsynaptic mitochondria isolated from YAC128 mice following acute application of brain cytosolic fractions from either WT or YAC128 animals. In **A** and **C**, representative traces of oxygen consumption by mitochondria treated with either WT concentrated cytosolic fraction (WT cf, blue traces) or YAC128 concentrated cytosolic fraction (HD cf, red traces). Where indicated, ADP (250μM in **A**, 150μM in **C**), 2,4-dinitrophenol (2,4-DNP, 60μM), and WT or YAC128 cytosolic fractions (WT cf or HD cf, 80μg of protein) were added to mitochondria. The incubation medium was supplemented with either 3 mM pyruvate (pyr) and 1 mM malate (mal) (**A**) or 3 mM succinate (succ) and 3

This article is protected by copyright. All rights reserved.

mM glutamate (glu) (**C**). In **B** and **D**, the statistical summary of respiratory rates of mitochondria incubated with either pyruvate plus malate (**B**) or succinate plus glutamate (**D**). Data are mean±SD, n=5 separate independent mitochondrial preparations.

Figure 4. Membrane potential of brain nonsynaptic mitochondria isolated from WT mice following acute application of brain cytosolic fractions from WT or YAC128 animals. In **A**-**C** and **E**-**G**, representative TPP^+ traces indicative of changes in mitochondrial membrane potential ($\Delta\psi$) in response to 250μM ADP and 60μM 2,4-dinitrophenol following addition of vehicle (10μL of Isolation Medium 1, green traces) (**A**, **E**), or cytosolic fractions from either WT (WT cf, blue traces) (**B**, **F**) or YAC128 (HD cf, red traces) (**C**, **G**) mice. In **A**-**C**, the standard incubation medium was supplemented with 3 mM pyruvate (pyr) and 1 mM malate (mal). In **E**-**G**, the standard incubation medium was supplemented with 3 mM succinate (succ) and 3 mM glutamate (glu). In **D** and **H**, statistical summaries of mitochondrial membrane potential measurements taken 30 seconds prior to ADP addition in the standard incubation medium containing pyruvate plus malate or succinate plus glutamate, respectively. Data are mean±SD, n=4 separate independent mitochondrial preparations.

Figure 5. Membrane potential of brain nonsynaptic mitochondria isolated from YAC128 mice following acute application of brain cytosolic fractions from WT and YAC128 animals. In **A**-**D**, representative TPP^+ traces indicative of changes in mitochondrial membrane potential ($\Delta\psi$) in response to 250μM ADP and 60μM 2,4-dinitrophenol following addition of brain cytosolic fractions from either WT (WT cf, blue traces) (**A**, **C**), or YAC128 (HD cf, red traces) (**B**, **D**) mice. In **A**-**B**, the standard incubation medium was supplemented with 3 mM pyruvate (pyr) and 1 mM malate (mal). In **C**-**D**, the standard incubation medium was supplemented with 3 mM succinate (succ) and 3 mM glutamate (glu). In **E** and **F**, statistical summaries of mitochondrial membrane potential measured 30 seconds prior to ADP addition in the standard incubation medium containing pyruvate plus malate or succinate plus glutamate, respectively. Data are mean±SD, n=4 separate independent mitochondrial preparations.

Figure 6. H_2O_2 production by brain nonsynaptic mitochondria isolated from WT mice following acute application of brain cytosolic fractions from WT or YAC128 animals. In **A** and **B**, H_2O_2 production by brain mitochondria isolated from WT mice before and after the addition of vehicle (10μL of Isolation Medium 1, green traces) or brain cytosolic fractions from either WT (WT cf, blue traces) or YAC128 (HD cf, red traces) mice. H_2O_2 production was assessed using an Amplex Red assay (Molecular Probes) with mitochondria incubated in the standard incubation medium supplemented with either 3 mM pyruvate (pyr) and 1 mM malate (mal) (**A**) or 3 mM succinate (succ) and 3 mM glutamate (glu) (**B**). In **C** and **D**, statistical summaries of mitochondrial H_2O_2 production rate. Data are mean±SD, n=4 separate independent mitochondrial preparations.

Figure 7. H_2O_2 production by brain nonsynaptic mitochondria isolated from YAC128 mice following acute application of brain cytosolic fractions from WT or YAC128 animals. In **A** and **B**, H_2O_2 production by brain mitochondria isolated from YAC128 mice before and after the addition of brain cytosolic fractions from either WT (WT cf, blue traces) or YAC128 (HD cf, red traces) mice. H_2O_2 production was assessed using an Amplex Red assay (Molecular Probes) with mitochondria incubated in the standard incubation medium supplemented with either 3 mM pyruvate (pyr) and 1 mM malate (mal) (**A**) or 3 mM succinate (succ) and 3 mM glutamate (glu) (**B**). In **C** and **D**, statistical summaries of

Accepted Article

This article is protected by copyright. All rights reserved.

mitochondrial H_2O_2 production rate. Data are mean±SD, n=4 separate independent mitochondrial preparations.

Figure 8. Ca^{2+} uptake capacity of brain nonsynaptic mitochondria isolated from WT and YAC128 mice following acute application of brain cytosolic fractions from WT or YAC128 animals. In **A** and **C**, Ca^{2+} uptake capacity of brain mitochondria from either WT or YAC128 mice, respectively, following addition of cytosolic fractions from either WT (WT cf, blue traces) or YAC128 (HD cf, red traces) mice. The standard incubation medium was supplemented with 0.1 mM ADP and 1µM oligomycin (Chalmers and Nicholls 2003). In **A**, control with vehicle (10µL of Isolation Medium 1, green trace) is shown. Ca^{2+} uptake was assessed with a miniature Ca^{2+}-selective electrode as a decrease in Ca^{2+} concentration in the standard incubation medium supplemented with 3 mM pyruvate (pyr) and 1 mM malate (mal). In **B** and **D**, statistical summaries of Ca^{2+} uptake capacity of brain mitochondria from WT and YAC128 mice, respectively. Data are mean±SD, n=5 separate independent mitochondrial preparations.

Accepted Article

This article is protected by copyright. All rights reserved.

Accepted Article

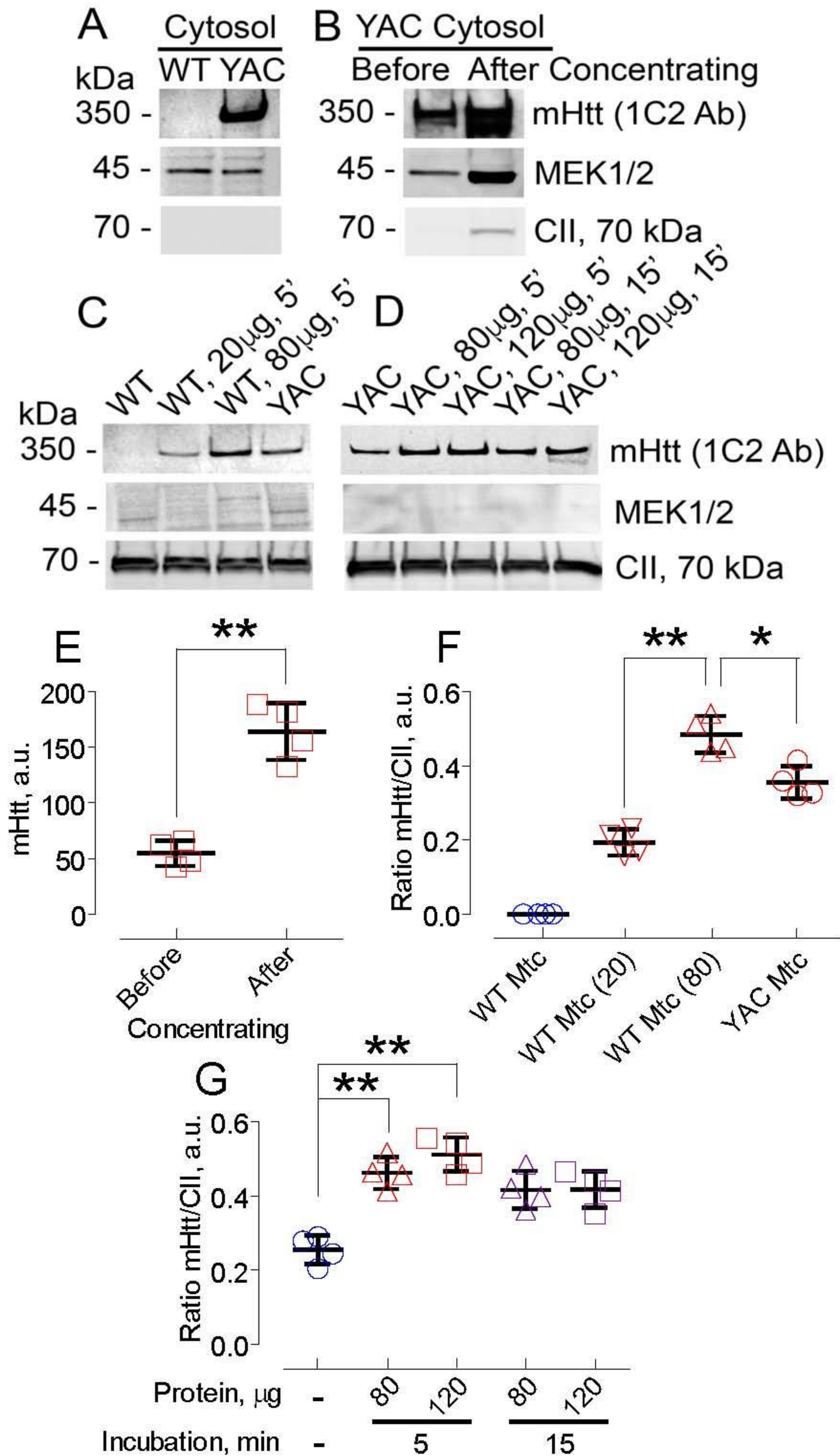

This article is protected by copyright. All rights reserved.

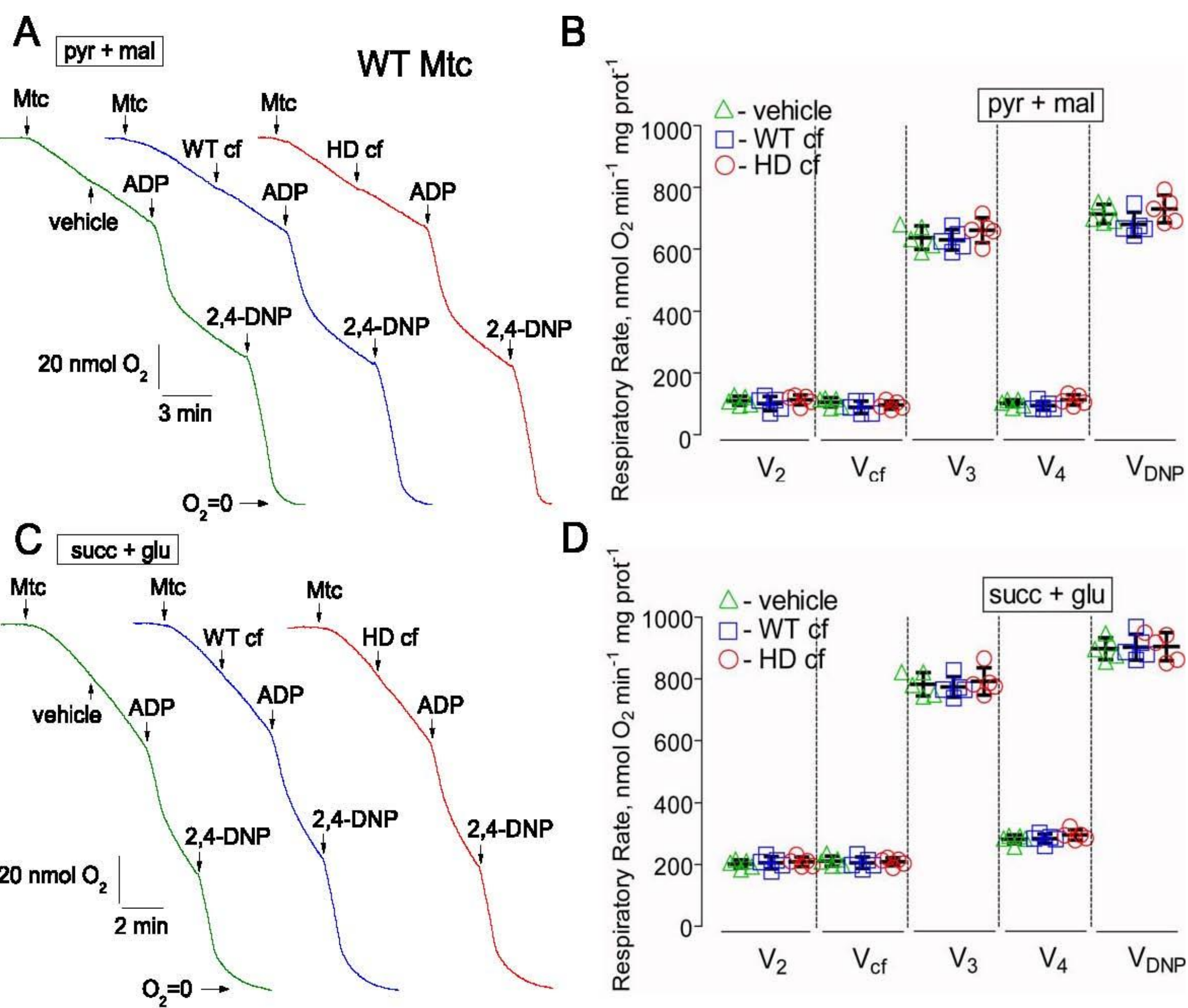

Accepted Article

This article is protected by copyright. All rights reserved.

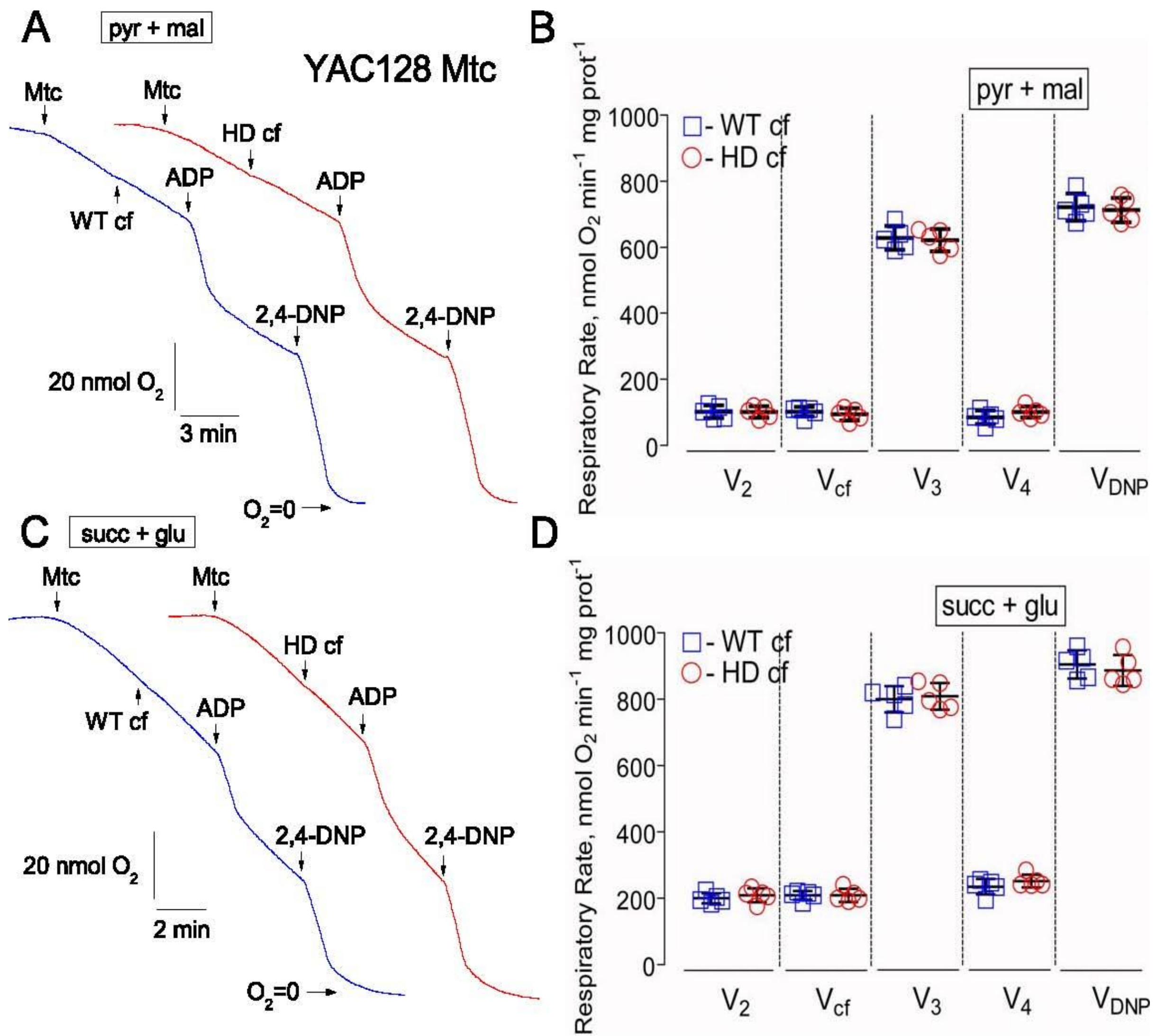

Accepted Article

This article is protected by copyright. All rights reserved.

Accepted Article

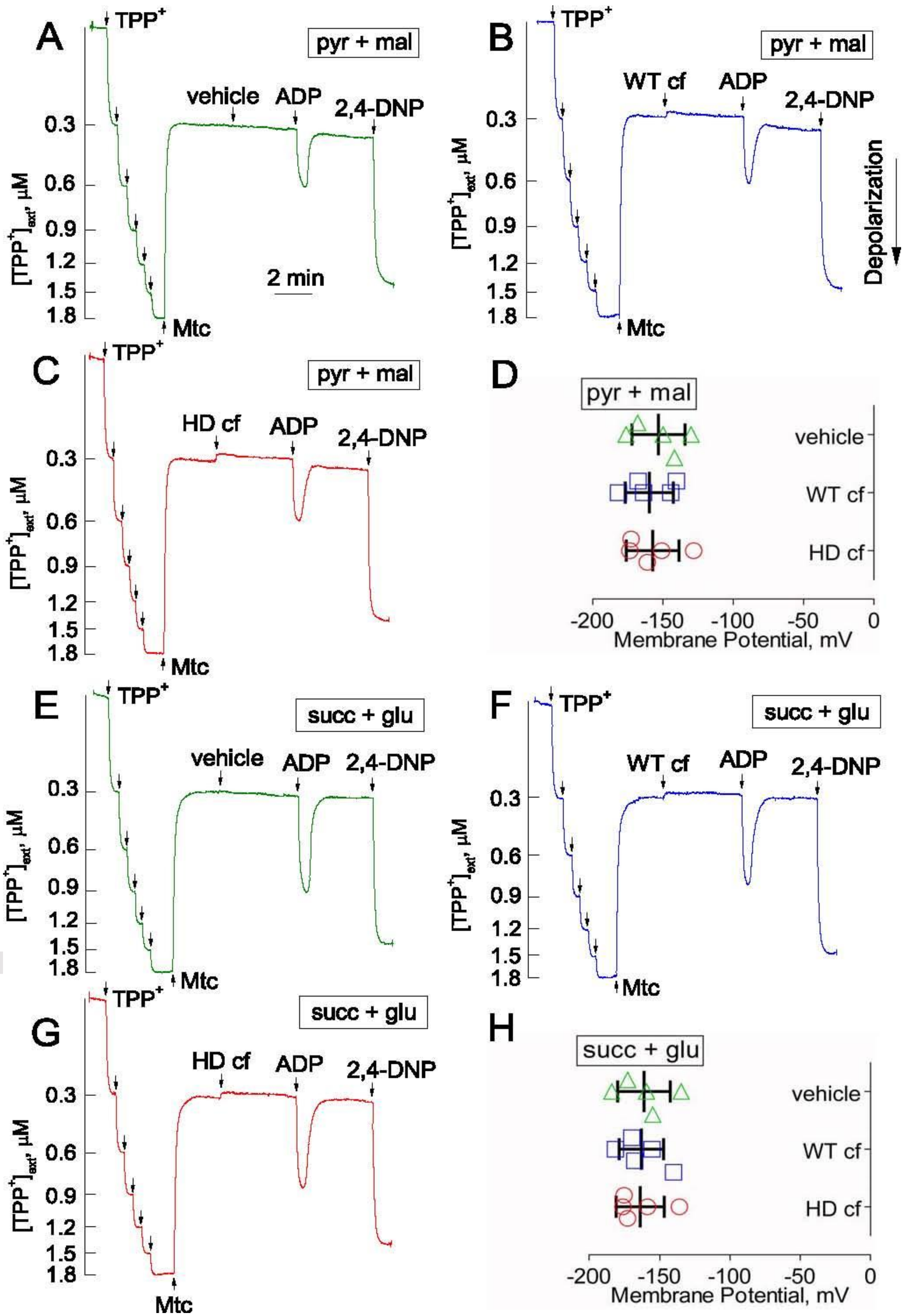

This article is protected by copyright. All rights reserved.

Accepted Article

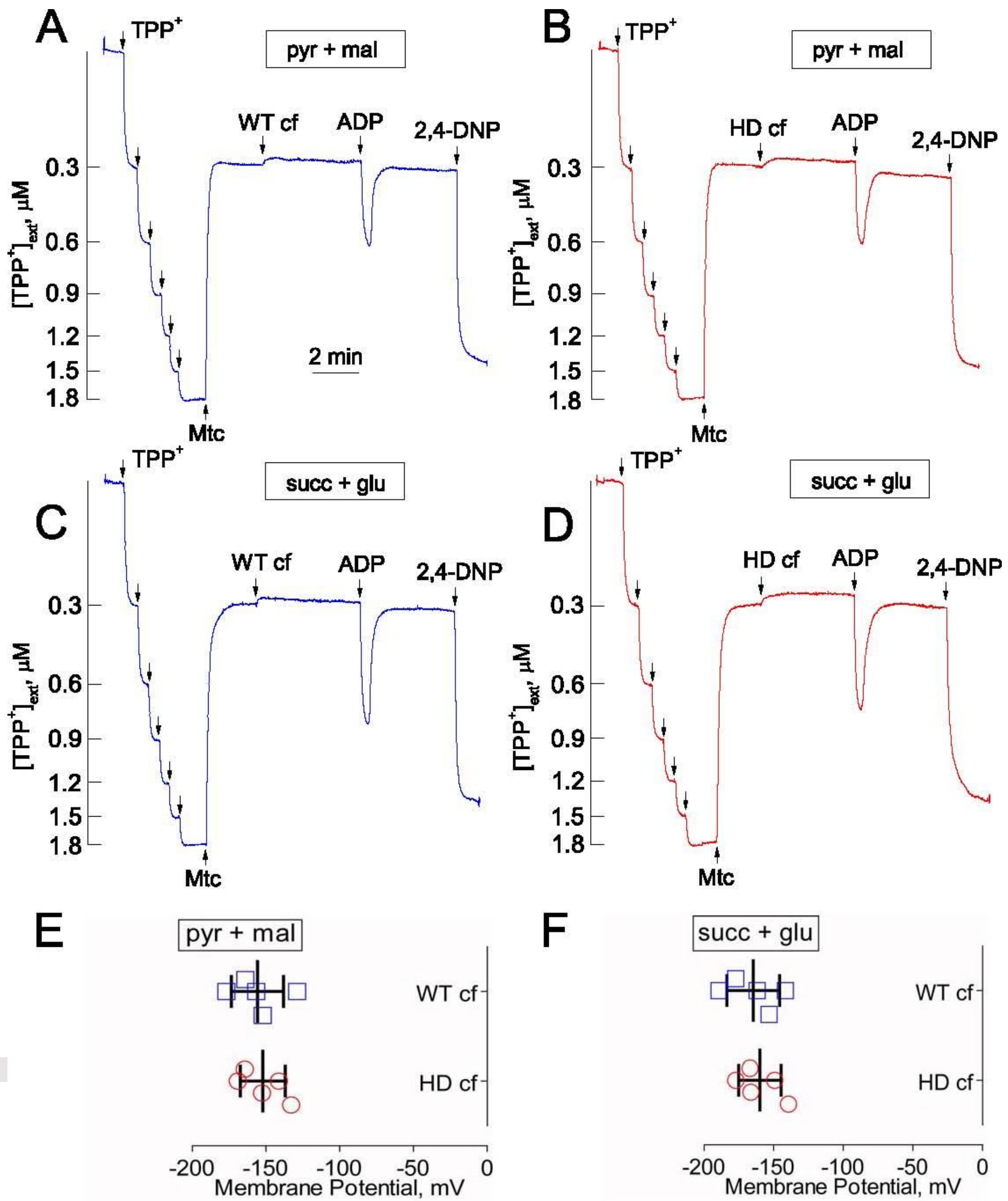

This article is protected by copyright. All rights reserved.

Accepted Article

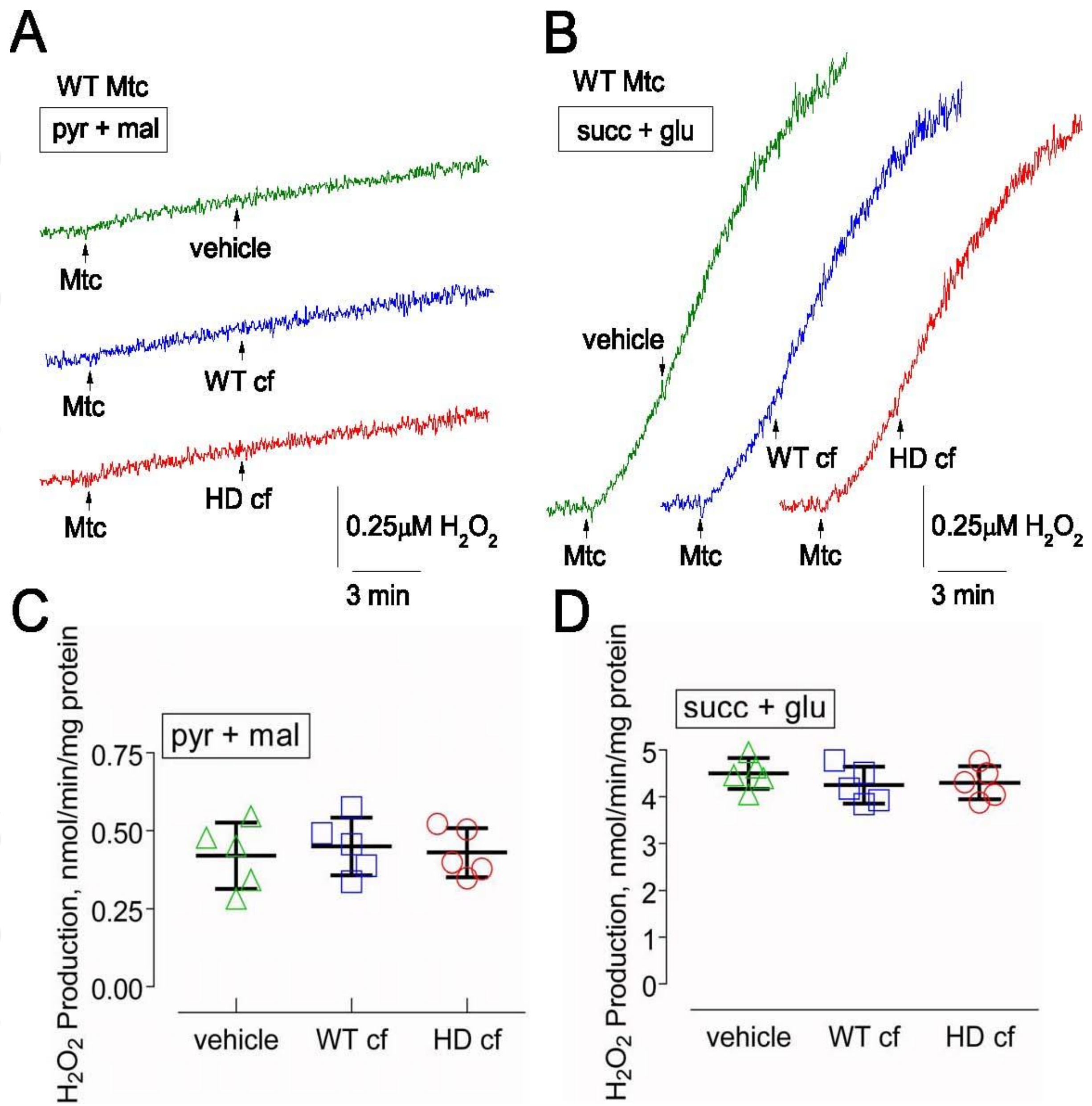

This article is protected by copyright. All rights reserved.

Accepted Article

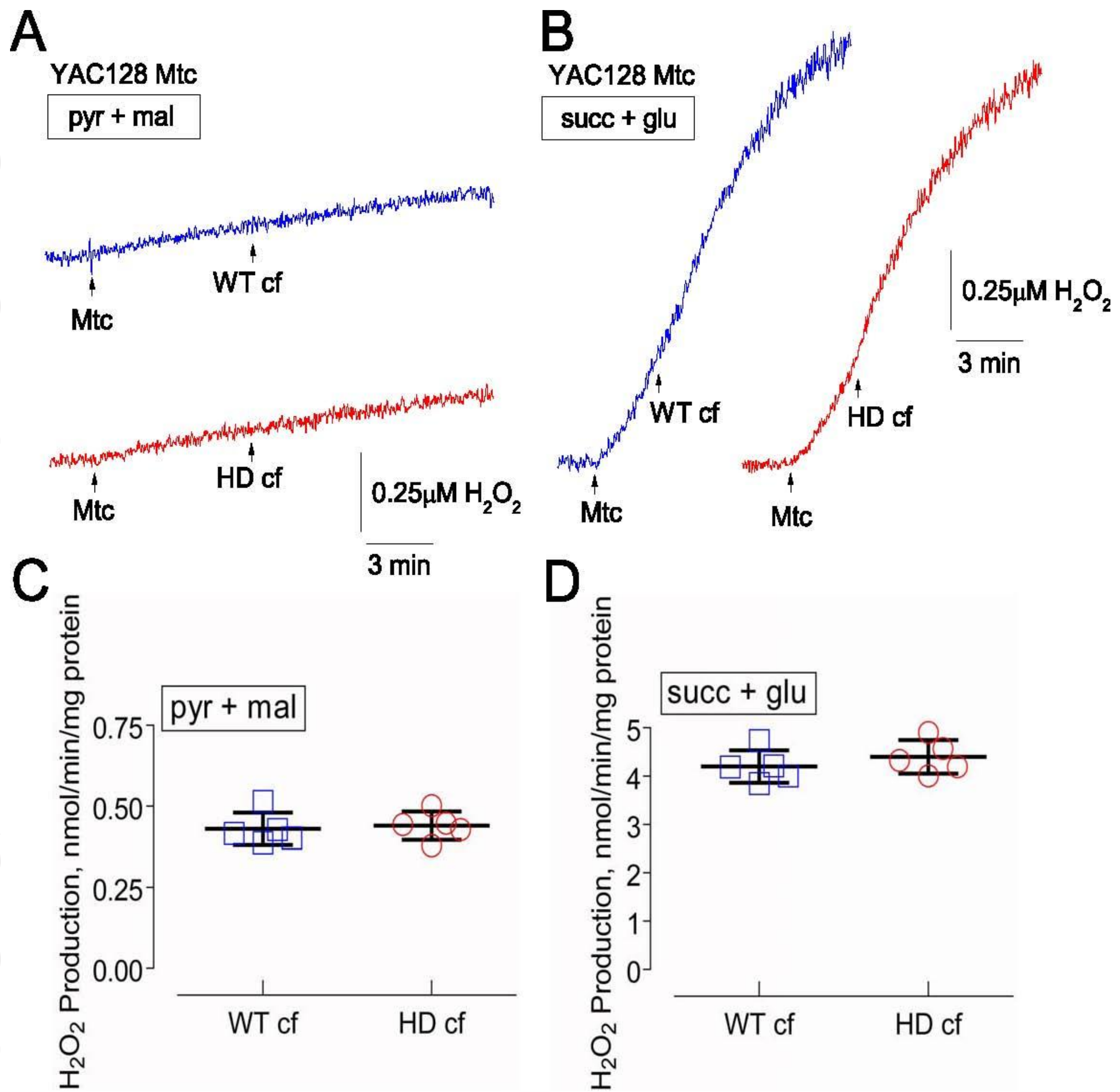

This article is protected by copyright. All rights reserved.

Accepted Article

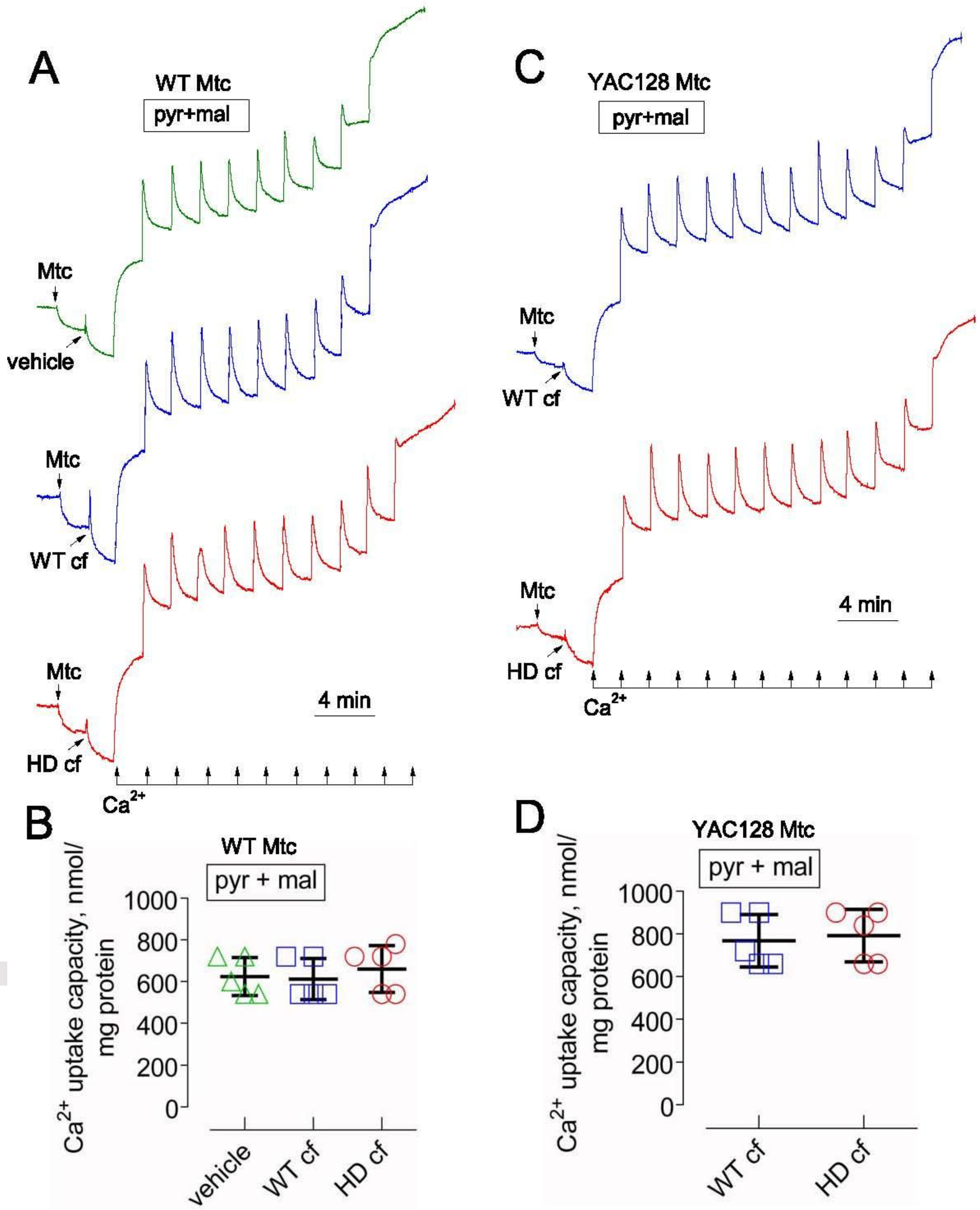

This article is protected by copyright. All rights reserved.